Ballistic electron waveguide adder

Michael G. Snyder and Linda E. Reichl
Center for Studies in Statistical Mechanics and Complex Systems, The University of Texas at Austin, Austin, Texas 78712, USA
(Received 1 July 2004; published 30 November 2004)

We analyze a quantum network, constructed with ballistic electron waveguides, which can add one-bit binary numbers. We consider two different adder networks, one constructed with Hadamard gates and the other constructed with $\sqrt{\text{NOT}}$ gates. Reflection of electron probability at the gates causes a loss in fidelity of the overall calculation. A fidelity requirement for the implementation of individual rotation gates corresponding to a probability $p>1/2$ of completing the addition successfully is found.

DOI: 10.1103/PhysRevA.70.052330 PACS number(s): 03.67.Mn, 03.65.Ud, 73.23.Ad

I. INTRODUCTION

Quantum computation using ballistic electron waveguides was first proposed by Ioniciou *et al.* [1] for a model in which electron wave packets are propagated through a waveguide network. In this model, two spatially separated waveguides are used to form a "flying qubit" giving the network a directionality. The spatial location of the electron in the dual-waveguide system corresponds to the state of the qubit. An electron is injected from the left into either the waveguide representing the state $|0\rangle$ or the waveguide representing the state $|1\rangle$. As the electron travels through the waveguide system, it encounters a gate region where over some length the potential barrier between the two waveguides is lowered. This allows the electron probability to distribute itself between both waveguides simultaneously as it continues to travel thus creating a linear superposition of the $|0\rangle$ and $|1\rangle$ qubit states. However, at the region of lowered potential some of the electron probability will be reflected back towards the input side of the device. Akguc *et al.* [2] have shown that when reflection is present in the system the dual-waveguide structures actually act as four state *quqits* instead of two state qubits (a quqit is a four-state system representing a quantum quaternary digit). They use a stationary state picture to analyze the network dynamics. This gives a more realistic picture of the waveguide network which, at low temperature, operates at the Fermi energy. They find that the gates can have resonances that minimize reflection and allow the production of entangled Bell states in simple waveguide networks. In this paper, we generalize the approach of Akguc *et al.* [2] and study the effects of reflection on a waveguide network which allows the addition of two one-bit numbers.

In order to perform simple addition we need to perform the analogy of single-qubit and two-qubit unitary transformations in our quqit system. The standard single-qubit unitary transformation used for quantum algorithms is the Hadamard gate [3]. A Hadamard gate is a rotation gate (which we denote as $\hat{H}$) that takes a state initially in the $|0\rangle$ or $|1\rangle$ states and rotates it into a equal linear superposition of the two states. Thus, $\hat{H}|1\rangle=(-|1\rangle+|0\rangle)/\sqrt{2}$ and $\hat{H}|0\rangle=(|1\rangle+|0\rangle)/\sqrt{2}$. The Hadamard gate has the property that $\hat{H}\hat{H}|1\rangle=|1\rangle$ and $\hat{H}\hat{H}|0\rangle=|0\rangle$. Akguc *et al.*, in their numerical experiments on the electron waveguide system, were able to construct a $\sqrt{\text{NOT}}$ gate. A $\sqrt{\text{NOT}}$ gate, similar to the Hadamard gate, takes a state initially in the $|0\rangle$ or $|1\rangle$ states and rotates it into an equal linear superposition of the two. A pure $\sqrt{\text{NOT}}$ gate, which we denote as $\hat{Q}'$, acts on the basis states $\hat{Q}'|1\rangle=-[(1+i)|1\rangle+(1-i)|0\rangle]/2$ and $\hat{Q}'|0\rangle=-[(1-i)|1\rangle+(1+i)|0\rangle]/2$ so that two applications of a $\sqrt{\text{NOT}}$ gate give $\hat{Q}'\hat{Q}'|0\rangle=|1\rangle$ and $\hat{Q}'\hat{Q}'|1\rangle=|0\rangle$. In order to keep the analysis of both the Hadamard and the $\sqrt{\text{NOT}}$ gates as similar as possible we study a gate, denoted as $\hat{Q}$, which behaves up to a phase as a pure $\sqrt{\text{NOT}}$ gate. This gate acts on the basis states $\hat{Q}|1\rangle=(|1\rangle-|0\rangle)/\sqrt{2}$ and $\hat{Q}|0\rangle=(|1\rangle+|0\rangle)/\sqrt{2}$ so that $\hat{Q}\hat{Q}|0\rangle=|1\rangle$ and $\hat{Q}\hat{Q}|1\rangle=-|0\rangle$. Computationally $\hat{Q}'$ and $\hat{Q}$ are equivalent. Much of the recent theory on quantum computation networks uses the Hadamard gate and in this paper we will study a simple adder network constructed using the Hadamard gate [4]. However, we will also show how to construct a simple adder network implementable with the $\sqrt{\text{NOT}}$ gate that can be realized in a semiconductor-based (GaAs/AlGaAs) electron waveguide network. We will then analyze the errors introduced into the final output states of these networks due to reflection at the rotation gates.

The standard two-qubit unitary transformation, the entanglement gate (also called the controlled phase gate), which we denote $\hat{V}$, acts on the two-qubit direct product space which consists of basis states $|1,\,1\rangle$, $|1,\,0\rangle$, $|0,\,1\rangle$, and $|0,\,0\rangle$. The entanglement gate that we consider here multiplies the state $|1,\,1\rangle$ by a factor of i. Thus, if the two-qubit state is $|\Phi\rangle=c_{1,1}|1,1\rangle+c_{1,0}|1,0\rangle+c_{0,1}|0,1\rangle+c_{0,0}|0,0\rangle$, where the coefficients c_{ij} $(j=0,1,\ i=0,1)$ are complex numbers, then $\hat{V}|\Phi\rangle=ic_{1,1}|1,1\rangle+c_{1,0}|1,0\rangle+c_{0,1}|0,1\rangle+c_{0,0}|0,0\rangle$. In the waveguide network, the entanglement gate can, in principle, be implemented using the Coulomb interaction between two electrons. A segment of the dielectric material between the states $|1\rangle$ of the two flying qubits is altered so that a potential is generated in both $|1\rangle$ waveguides due to the Coulomb force between a pair of electrons traveling in those waveguides. The dielectric material in the remainder of the waveguide network is not altered so electrons traveling in the $|0\rangle$ waveguides will not be affected by or affect other electrons. Therefore, an interaction occurs only when the electrons in each qubit are both traveling in the $|1\rangle$ waveguide. This interaction causes an overall phase shift on the $|1,\,1\rangle$

direct product state only. Reflection can also occur during the two-qubit controlled phase shift operation. However, these reflections differ from those of the rotation gate in that they occur in only the $|1\rangle$ waveguide and then only when there is electron probability in the $|1\rangle$ waveguide of the other qubit. The confinement of the reflections to a single waveguide and the conditional character of the reflections will introduce a new kind of error into the networks and also effect the output state of the system. However, the length of the interaction region and the distance between the $|1\rangle$ waveguides can be set such that a phase of $i=\sqrt{-1}$ is achieved [2], so we do not consider those reflections here.

The basic computation required to implement Shor's algorithm involves modular exponentiation [5]. A complex operation like modular exponentiation is realized by beginning with simple operations then combining them to form more complex operations. One way to perform modular exponentiation is to first find a network which performs simple addition, often referred to as an *adder*. The adder is then used to build a network for modular addition, which in turn is used to find a network for modular multiplication, and finally this is used to build the entire network for modular exponentiation [6]. There are two basic computational gates required for the implementation of these arithmetic networks. The simpler of the two gates acts on two qubits and is referred to as a *controlled-not* gate (CNOT gate). The CNOT gate negates one qubit conditional on the value of a neighboring qubit. The second gate acts on three qubits and is referred to as a *controlled-controlled-NOT* gate (C^2NOT gate). The C^2NOT gate negates one qubit conditional on the values of both neighboring qubits. All of the arithmetic operations necessary for the implementation of Shor's algorithm can be constructed with CNOT gates, C^2NOT gates, and simple single-qubit NOT gates. The simplest arithmetic operation combining these computational gates is the addition of two one-bit numbers which requires three qubits, one CNOT gate, and one C^2NOT gate. The addition of two two-bit numbers requires a minimum of six qubits, seven CNOT gates, and three C^2NOT gates. In general, the addition of two n-bit numbers requires $3n$ qubits, $4n+3$ CNOT gates, and $4n$ C^2NOT gates. The number of gates and qubits increases rapidly as the operations become more complex.

At low temperatures, $T\sim 0.1-2.0$ K, semiconductor-based ($GaAs/Al_{1-x}Ga_xAs$) electron waveguide networks have a phase coherence length of the order $L_\phi \sim 30-40$ μm [7]. Numerical experiments have shown that a single-qubit rotation gate as small as 0.17 μm in length can produce the desired linear superposition of states and simple models of the Coulomb coupler region require an interaction region of less than 0.4 μm [2,8]. In principle, the simple adder network is within the reach of current technologies [9]. More sophisticated networks involving large numbers of qubit transformations would require advancements in the materials used to construct ballistic electron waveguides. One-dimensional (1D) nanowires constructed of carbon nanotubes preserve electron phase coherence over micrometer lengths at room temperature and are possible candidates for the future implementation of such networks.

In subsequent sections, we focus on a quantum waveguide network that has the ability to add two one-bit numbers. We will show how to build the adder from either Hadamard gates or $\sqrt{\text{NOT}}$ gates. We will focus on the effect of the error caused by the reflection of electron probability at the Hadamard and $\sqrt{\text{NOT}}$ gates.

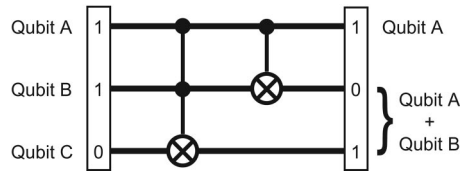

FIG. 1. A schematic of the simple adder. Qubit A is added to qubit B using qubit C as a carry bit. The answer of the addition operation is read schematically from bottom to top with the bottom qubit representing the most significant bit.

II. THE QUBIT ADDER

In this section we will describe the structure of an adder for the case of flying qubits (quqits with no reflection). A quantum adder takes as input two binary numbers and outputs two binary numbers. A binary number of length n is represented by a collection of n qubits, each of which takes on the value of $|0\rangle$ or $|1\rangle$. (Superpositions of $|0\rangle$ and $|1\rangle$, while valid inputs, complicate the discussion and do not need to be explicitly considered.) In general, when two n-qubit binary numbers are added they sum to an $(n+1)$-qubit binary number, e.g., $1011+1100=10111$. Therefore, an extra set of qubits, called *carry qubits*, also need to be included. If we denote two n-qubit numbers as n_1 and n_2, and a quantum adder as $\hat{O}_{add}$, then the action of the adder on the two inputs is $\hat{O}_{add}|n_1\rangle|n_2\rangle=|n_1\rangle|n_1+n_2\rangle$, where the state $|n_i\rangle$ denotes a direct product state consisting of n individual qubit states.

We study the simplest version of a quantum adder which adds two n-qubit numbers with $n=1$. The computation requires three qubits: two qubits to represent the two one-qubit numbers, and one carry qubit. We label the three qubits A, B, and C as shown in Fig. 1. A single electron is injected into each qubit on the left and all three electrons travel to the right through a series of gates. The states of the electrons are determined when they emerge on the right. Our analysis involves the construction of a quantum network which can perform the addition of two one-digit binary numbers to give one two-digit binary numbers: $1+1=10$; $1+0=01$; $0+1=01$; and $0+0=00$. We will focus on the case $1+1=10$ (one+one=two). An electron enters qubit A in state $|\phi_A^l\rangle=|1\rangle$, qubit B in state $|\phi_B^l\rangle=|1\rangle$, and qubit C in state $|\phi_C^l\rangle=|0\rangle$. The number represented by the state of qubit A is added to that represented by qubit B, using qubit C as a carry qubit. The initial state of the computer is therefore $|\Phi^l\rangle=|\phi_A^l,\phi_B^l,\phi_C^l\rangle=|1,1,0\rangle$. In our adder, the state of qubit A should remain unchanged and the summation of the numbers represented by qubits A and B is a two-qubit number whose individual digits are represented by the states of qubits C and B, with qubit C representing the most significant bit. Therefore, the final state of our computer should be $|\Phi^r\rangle=|1,0,1\rangle$, where the answer of the addition, 10, is represented by qubits C and B read in that order.

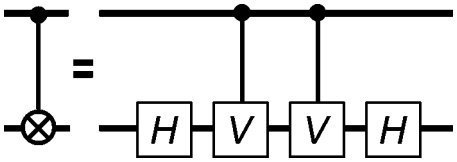

FIG. 2. A schematic of the CNOT gate. The Hadamard gates are represented by *H*'s and the controlled phase gates are represented by *V*'s.

The quantum adder network, using either the Hadamard or $\sqrt{\text{NOT}}$ gates, is drawn schematically in Fig. 1 in terms of the complex two-qubit CNOT gate, denoted as $\hat{G}_2$, and the complex three-qubit C^2NOT gate, denoted as $\hat{G}_3$. The CNOT gate $\hat{G}_2$ flips the state of one qubit—the *target* qubit—conditional on the state of another qubit—the *control* qubit. The state of the target qubit will flip only if the state of the control qubit is $|1\rangle$. The C^2NOT gate $\hat{G}_3$ flips the state of a target qubit conditional on the states of *two* control qubits. The target qubit flips only if the state of *both* control qubits is $|1\rangle$. The gates $\hat{G}_2$ and $\hat{G}_3$ are defined differently depending on whether one uses Hadamard or $\sqrt{\text{NOT}}$ gates. The output state is obtained from the input state by the action of these two complex gates such that $|\Phi^r\rangle = \hat{G}_2\hat{G}_3|\Phi^l\rangle$. The definitions of $\hat{G}_2$ and $\hat{G}_3$ in terms of Hadamard gates and entanglement gates are shown in Figs. 2 and 3. The definitions of $\hat{G}_2$ and $\hat{G}_3$ in terms of $\sqrt{\text{NOT}}$ gates and entanglement gates are shown in Figs. 4 and 5.

The order of the $\sqrt{\text{NOT}}$ gates in certain areas of the network allows for a contraction in the overall number of gates in the network. In $\hat{G}_2$ three $\sqrt{\text{NOT}}$ gates fall in a row amounting to three successive rotations of the qubit. In ballistic electron waveguide qubits it is possible to perform all three rotations with only one gate where the new gate $(\hat{Q})^3$ is simply three times longer than the original $\sqrt{\text{NOT}}$ gate. We show the $\sqrt{\text{NOT}}$ network here as a collection of only two types of gates but in the analysis we treat the gate $(\hat{Q})^3$ as a single gate.

III. QUQIT OPERATIONS

The overall structure of the adder described in Sec. II applies to the quantum network when reflection is allowed to occur at the gates. However, the qubits become ququits and the gates act on a larger state space. Below we describe the adder network formed from three ququits. We follow as closely as possible the notation in Ref. [2].

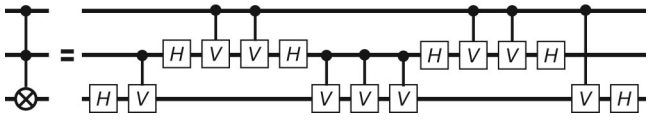

FIG. 3. A schematic of the C^2NOT gate. The Hadamard gates are represented by *H*'s and the controlled phase gates are represented by *V*'s.

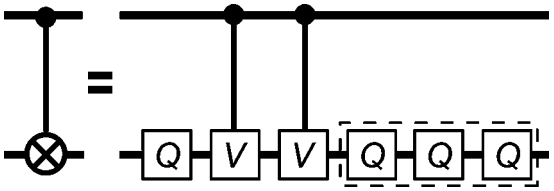

FIG. 4. A schematic of the CNOT gate using $\sqrt{\text{NOT}}$ gates. The $\sqrt{\text{NOT}}$ gates are represented by *Q*'s and the controlled phase gates are represented by *V*'s. The dashed box indicates the three $\sqrt{\text{NOT}}$ gates that can be consolidated into a single gate by making the gate three times longer.

In the quqit network, electrons can flow from left to right or from right to left due to reflection at the gates. We denote the states of electrons in quqit *A* that travel to the right (left) in the upper and lower leads as $|1\rangle_A$ and $|0\rangle_A$ ($|u\rangle_A$ and $|d\rangle_A$), respectively. Similarly, we denote the analogous states in quqit *B* as $|1\rangle_B$ and $|0\rangle_B$ ($|u\rangle_B$ and $|d\rangle_B$), respectively, and in quqit *C* they are denoted $|1\rangle_C$ and $|0\rangle_C$ ($|u\rangle_C$ and $|d\rangle_C$), respectively.

Because of the gates, the electron probability amplitudes in the various segments of a given quqit will vary as the electrons traverse the network from left to right. Probability amplitudes for *right-flowing* electrons will have subscripts 1 and 0 and probability amplitudes for *left-flowing* electrons will have subscripts *u* and *d*.

We will introduce specific notation for the probability amplitudes on the left-hand side of each quqit and on the right-hand side of each quqit as follows. *Quqit A*: probability amplitudes for states $|1\rangle_A$ and $|0\rangle_A$ ($|u\rangle_A$ and $|d\rangle_A$) *entering* quqit *A* on the left (right) are denoted a_1 and a_0 (e_u and e_d), respectively; probability amplitudes for states $|u\rangle_A$ and $|d\rangle_A$ ($|1\rangle_A$ and $|0\rangle_A$) *leaving* quqit *A* on the left (right) are denoted a_u and a_d (e_1 and e_0), respectively. *Quqit B*: probability amplitudes for states $|1\rangle_B$ and $|0\rangle_B$ ($|u\rangle_B$ and $|d\rangle_B$) *entering* quqit *B* on the left (right) are denoted b_1 and b_0 (f_u and f_d), respectively; probability amplitudes for states $|u\rangle_B$ and $|d\rangle_B$ ($|1\rangle_B$ and $|0\rangle_B$) *leaving* quqit *B* on the left (right) are denoted b_u and b_d (f_1 and f_0), respectively. *Quqit C*: probability amplitudes for states $|1\rangle_C$ and $|0\rangle_C$ ($|u\rangle_C$ and $|d\rangle_C$) *entering* quqit *C* on the left (right) are denoted c_1 and c_0 (g_u and g_d), respectively; probability amplitudes for states $|u\rangle_C$ and $|d\rangle_C$ ($|1\rangle_C$ and $|0\rangle_C$) *leaving* quqit *C* on the left (right) are denoted c_u and c_d (g_1 and g_0), respectively.

Each quqit individually conserves electron probability and electrons in different quqits are distinguishable. The conditions for electron probability conservation on each of the quqits are as follows: for quqit *A*,

$$|a_1|^2 + |a_0|^2 + |e_u|^2 + |e_d|^2 = |a_u|^2 + |a_d|^2 + |e_1|^2 + |e_0|^2; \quad (1)$$

for quqit *B*,

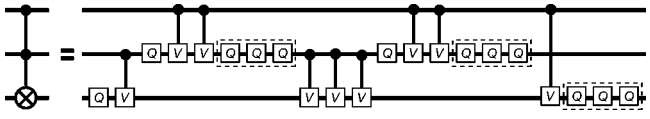

FIG. 5. A schematic of the C^2NOT gate using $\sqrt{\text{NOT}}$ gates. The $\sqrt{\text{NOT}}$ gates are represented by *Q*'s and the controlled phase gates are represented by *V*'s. The dashed boxes indicate the sets of three $\sqrt{\text{NOT}}$ gates that can be consolidated into single gates.

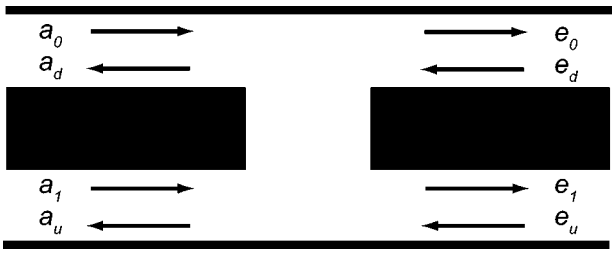

FIG. 6. A schematic of the Hadamard gate. Two ballistic electron waveguides are coupled by lowering the potential barrier between them. An electron traveling initially in a single waveguide will be found in either waveguide with equal probability after crossing the gate. The value a_k represents the probability amplitude on the left of the gate in the kth state, e_k represents the probability amplitude on the right of the gate in the kth state.

$$|b_1|^2 + |b_0|^2 + |f_u|^2 + |f_d|^2 = |b_u|^2 + |b_d|^2 + |f_1|^2 + |f_0|^2; \quad (2)$$

and for quqit C,

$$|c_1|^2 + |c_0|^2 + |g_u|^2 + |g_d|^2 = |c_u|^2 + |c_d|^2 + |g_1|^2 + |g_0|^2. \quad (3)$$

As described in [2], we can build the dynamics of the adder network out of the scattering matrices (S matrices) of the individual gates. The S matrix for a rotation gate in quqit A, for example (see Fig. 6), connects the column matrix of incoming probability amplitudes, $\psi_{in}=(a_1,a_0,e_u,e_d)^T$, to the column matrix of outgoing probability amplitudes, $\psi_{out}=(a_u,a_d,e_1,e_0)^T$. We can write an S matrix for each of the rotation gates in the form

$$S = \begin{pmatrix} r_{u,1} & r_{u,0} & t_{u,u} & t_{u,d} \\ r_{d,1} & r_{d,0} & t_{d,u} & t_{d,d} \\ t_{1,1} & t_{1,0} & r_{1,u} & r_{1,d} \\ t_{0,1} & t_{0,0} & r_{0,u} & r_{0,d} \end{pmatrix}, \quad (4)$$

where t_{ij} is the probability amplitude for an electron entering the gate in state $|j\rangle$ $(j=1,0,u,d)$ to be transmitted into the state $|i\rangle$ $(i=1,0,u,d)$, and r_{ij} is the probability amplitude for an electron entering the gate in state $|j\rangle$ $(j=1,0,u,d)$ to be reflected into the state $|i\rangle$ $(i=1,0,u,d)$. We can generalize the Hadamard and $\sqrt{\text{NOT}}$ gates to include the possibility of reflection. For the generalized Hadamard gate, we let S_H denote the S matrix and we write

$$t_{uu} = t_{ud} = t_{du} = t_{11} = t_{01} = t_{10} = \frac{1-b}{\sqrt{2}},$$

$$t_{dd} = t_{00} = \frac{-(1-b)}{\sqrt{2}},$$

$$r_{u0} = r_{0u} = b,$$

$$r_{d1} = r_{1d} = -b,$$

$$r_{u1} = r_{d0} = \sqrt{2}\sqrt{b-b^2},$$

$$r_{1u} = r_{0d} = -\sqrt{2}\sqrt{b-b^2}, \quad (5)$$

and for the generalized $\sqrt{\text{NOT}}$ gate we let S_Q denote the S matrix and we write

$$t_{11} = t_{10} = t_{00} = t_{dd} = t_{du} = t_{uu} = \frac{1-b}{\sqrt{2}},$$

$$t_{01} = t_{du} = \frac{-(1-b)}{\sqrt{2}},$$

$$r_{0u} = r_{d1} = b,$$

$$r_{1d} = r_{u0} = -b,$$

$$r_{d0} = r_{u1} = \sqrt{2}\sqrt{b-b^2},$$

$$r_{1u} = r_{0d} = -\sqrt{2}\sqrt{b-b^2}, \quad (6)$$

where b is a real parameter which determines the amount of reflection at the gate. We also write an S matrix for the areas in the network where three $\sqrt{\text{NOT}}$ gates can be consolidated into one gate, $(\sqrt{\text{NOT}})^3$, which we denote simply as $(S_Q)^3$

$$t_{00} = t_{10} = t_{11} = t_{dd} = t_{ud} = t_{uu} = \frac{1-b}{\sqrt{2}},$$

$$t_{01} = t_{du} = \frac{-(1-b)}{\sqrt{2}},$$

$$r_{1u} = r_{d0} = b,$$

$$r_{0d} = r_{u1} = -b,$$

$$r_{d1} = r_{u0} = \sqrt{2}\sqrt{b-b^2},$$

$$r_{0u} = r_{1d} = -\sqrt{2}\sqrt{b-b^2}. \quad (7)$$

When $b=0$, the gate in Eq. (5) reduces to a pure Hadamard gate with no reflection, and the gate in Eq. (6) reduces to a pure $\sqrt{\text{NOT}}$ gate to within an overall phase. Both gates are parametrized so that as b is varied from 0 to 1 (total transmission to total reflection) the S matrix it remains unitary.

The S matrix acts on a state containing information about the state of the quqit on both sides of the gate. In constructing the adder network dynamics, we need to first construct the transfer matrix for each gate. The transfer matrix connects the probability amplitude on the left side of the gate to the probability amplitude on the right side of the gate. For example, for quqit A, it connects the column matrix $(a_1,a_0,a_u,a_d)^T$ on the left to the column matrix $(e_1,e_0,e_u,e_d)^T$. The transfer matrix can be constructed from the S matrix. We first define two "swapping" matrices λ and γ defined as

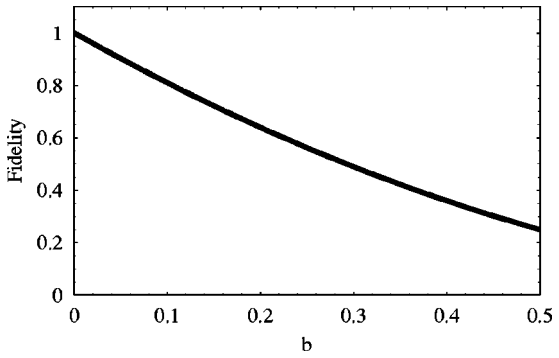

FIG. 7. The fidelity of the Hadamard gate as the reflection parameter is increased. Calculations for the single Hadamard gate and the entire network are carried out to $b=0.5$. Due to the similarity in parametrization, the fidelity profile of a $\sqrt{\text{NOT}}$ gate is identical.

$$\lambda = \begin{pmatrix} 1 & 0 & 0 & 0 \\ 0 & 1 & 0 & 0 \\ 0 & 0 & 0 & 0 \\ 0 & 0 & 0 & 0 \end{pmatrix}, \quad \gamma = I - \lambda = \begin{pmatrix} 0 & 0 & 0 & 0 \\ 0 & 0 & 0 & 0 \\ 0 & 0 & 1 & 0 \\ 0 & 0 & 0 & 1 \end{pmatrix}. \quad (8)$$

We can now express the transfer matrix T in terms of the S matrix and the swapping matrices,

$$T = (\gamma + \lambda \cdot S) \cdot (\lambda + \gamma \cdot S)^{-1}. \quad (9)$$

Given an input of unit probability in state $|1\rangle$ of a given quqit, a perfect Hadamard gate will produce an output of $|\phi_0\rangle = (1/\sqrt{2})(|0\rangle - |1\rangle)$. We can compare the output of a perfect Hadamard gate, $|\phi_0\rangle$, with the output $|\phi\rangle$ of an imperfect Hadamard gate with $b \neq 0$, by computing the fidelity of the gate,

$$F = |\langle \phi_0 | \phi \rangle|^2. \quad (10)$$

The fidelity of the gate decreases as b increases (see Fig. 7). Due to the similar structure of the $\sqrt{\text{NOT}}$ gate, its fidelity profile is identical to that of the Hadamard gate as the error parameter b is increased.

The perfect entanglement gate adds a phase of i to the $|1, 1\rangle$ state in the two-qubit direct product space. In case of two *quqits* there is also the possibility that the electrons will travel through the coupling region towards the input side. The direct product space of two quqits has 16 orthogonal states. Two of these 16 states ($|1, 1\rangle$ and $|u,u\rangle$) correspond to the case of two electrons traveling through the entanglement gate at the same time and in the same direction. We will limit our analysis to the case where the entanglement gate functions without reflection, but we will include the additional possibility that the electrons can be traveling toward the input side of the network. Thus, we will work with an entanglement gate that multiplies both of the states $|1, 1\rangle$ and the $|u,u\rangle$ by a phase of $i = \sqrt{-1}$. The matrix representing the entanglement gate V_{IJ} (where $I,J=A,B,C$ and $I \neq J$) is diagonal, differing from the 16×16 identity matrix only in the places indicated above where the matrix elements take the value of $i = \sqrt{-1}$.

IV. THE QUQIT ADDER

The sequence of gate operations used to add two quqits together is identical to that of the qubit adder. The gate operations themselves must be generalized to act on the four-state quqits. The network consists of quqits *A*, *B*, and *C*. Quqit *A* is added to quqit *B* and quqit *C* is used as a carry bit. The quqit adder is an entangled network. A general input or output state will be some superposition of the 64 orthogonal basis states $|i,j,k\rangle$ (where $i,j,k=1,0,u,d$) that can be formed from the states of the three quqits *A*, *B*, *C* (in that order). At any horizontal position along the adder, the state of the network can be written in the form

$$|\Psi\rangle = \phi_{111}|1,1,1\rangle + \phi_{110}|1,1,0\rangle + \phi_{11u}|1,1,u\rangle + \phi_{11d}|1,1,d\rangle + \phi_{101}|1,0,1\rangle + \cdots + \phi_{ddu}|d,d,u\rangle + \phi_{ddd}|d,d,d\rangle. \quad (11)$$

The input state (on the left) of the network is $|\Psi^l\rangle = |1,1,0\rangle$. In the limit of a perfect Hadamard or a perfect $\sqrt{\text{NOT}}$ gate, the output (on the right) is $|\Psi^r\rangle = |1,0,1\rangle$.

We study the effects of reflection at the Hadamard gates on the adder computation by constructing a matrix which describes the entire adder quantum network. This matrix acts on an input state (on the left) of the network and gives an output state (on the right). The input state and output states are written in the direct product basis of the three quqits [see Eq. (11)] and have 64 elements. The transfer matrices for the entire adder quantum network, acting on individual quqits, are generalized to the 64×64 matrices,

$$\mathbf{T}_A = T_A \otimes I_B \otimes I_C, \ \mathbf{T}_B = I_A \otimes T_B \otimes I_C, \ \mathbf{T}_C = I_A \otimes I_B \otimes T_C. \quad (12)$$

There are three distinct entanglement gates between the different quqits. Each transfer matrix representing an entanglement gate is diagonal, differing from the 64×64 identity matrix only where the two quqits acted upon both have

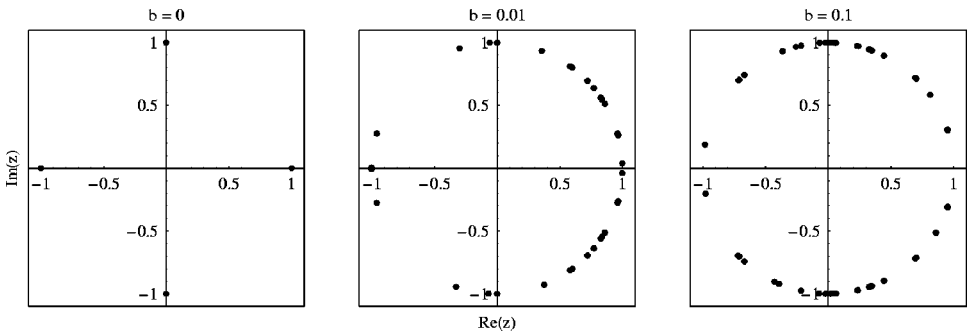

FIG. 8. The eigenvalues of **U** are plotted on the unit circle. At $b=0$ the eigenvalues are highly degenerate. As b is increased the eigenvalues spread throughout the unit circle rapidly. The unitary matrix corresponding to an adder network with the $\sqrt{\text{NOT}}$ gate shows a similar eigenvalue spreading.

the value of $|1\rangle$ or $|u\rangle$. For example, the entanglement transfer matrix acting on quqits A and C, $\mathbf{V}_{AC}$, is diagonal with a value of i in the entries $|1,0,1\rangle\langle 1,0,1|$, $|1,1,1\rangle\langle 1,1,1|$, $|1,u,1\rangle\langle 1,u,1|$, $|1,d,1\rangle\langle 1,d,1|$, $|u,1,u\rangle\langle u,1,u|$, $|u,0,u\rangle\langle u,0,u|$, $|u,d,u\rangle\langle u,d,u|$, and $|u,u,u\rangle\langle u,u,u|$, and 1's elsewhere.

With Hadamard gates defined on all three quqits and three entanglement gates defined between the pairs of quqits we now write the matrix corresponding to the action of the entire computation on an input state

$$\mathbf{T}^H_{add} = \mathbf{T}_B \cdot (\mathbf{V}_{AB})^2 \cdot \mathbf{T}_B \cdot \mathbf{T}_C \cdot \mathbf{V}_{AC} \cdot \mathbf{T}_B \cdot (\mathbf{V}_{AB})^2 \cdot \mathbf{T}_B \cdot (\mathbf{V}_{BC})^3 \cdot \mathbf{T}_B \cdot (\mathbf{V}_{AB})^2 \cdot \mathbf{T}_B \cdot \mathbf{V}_{BC} \cdot \mathbf{T}_C. \tag{13}$$

$\mathbf{T}^H_{add}$ represents the transfer matrix for the entire network. It acts on any general input state (on the left) written in a three-quqit combined basis and gives the output state (on the right) in that basis. The reflection parameter b is kept the same for all the Hadamard gates in the network.

The adder for the $\sqrt{\text{NOT}}$ gate network is given by

$$\mathbf{T}^Q_{add} = (\mathbf{T}_B)^3 \cdot (\mathbf{V}_{AB})^2 \cdot \mathbf{T}_B \cdot (\mathbf{T}_C)^3 \cdot \mathbf{V}_{AC} \cdot (\mathbf{T}_B)^3 \cdot (\mathbf{V}_{AB})^2 \cdot \mathbf{T}_B \cdot (\mathbf{V}_{BC})^3 \cdot (\mathbf{T}_B)^3 \cdot (\mathbf{V}_{AB})^2 \cdot \mathbf{T}_B \cdot \mathbf{V}_{BC} \cdot \mathbf{T}_C, \tag{14}$$

where $(\mathbf{T}_i)^3$ is the transfer matrix for a single gate which has the same effect as the $(\sqrt{\text{NOT}})^3$ gate. The $(\mathbf{T}_i)^3$ gate was given its own parametrization in Eq. (7).

A. The unitary matrix

In a computation using an actual semiconductor-based electron waveguide, one must work with the input and output states. However, the input and output states are unwieldy objects. $\mathbf{T}_{add}$, being a transfer matrix, is not unitary and does not preserve the norm of the states upon which it acts. Any acceptable solution must conserve probability in the individual quqits and it is difficult to impose this restriction using input states and output states. However, starting from $\mathbf{T}_{add}$ it is possible to find a unitary matrix which explicitly conserves electron probability.

In a manner similar to changing from the S matrix to the transfer matrix for a single Hadamard gate we swap entries from input and output states. The entries which we swap are found from the individual probability conservation equations Eqs. (1), (2), and (3). A column matrix representing an unentangled input state on the left side of the network, $|\Psi^l\rangle$, will contain amplitudes consisting of multiples of the individual probability amplitudes a_i, b_j, c_k. A column matrix representing an unentangled output state on the right side of the network, $|\Psi^r\rangle$, will contain amplitudes consisting of multiples of the individual probability amplitudes e_i, f_j, g_k. Rearranging Eqs. (1), (2), and (3) and multiplying them together gives a single probability conservation equation [see Eq. (A1) in the Appendix] consisting of multiples of coefficients which are found in the input and output states. We can use Eq. (A1) to identify states that will have the same norm. (This method is also valid when the input and output states are entangled, the situation encountered in the quqit adder network when reflection is present.) We first take the input state and decide according to the probability conservation equation which entries to keep and which to swap with the output state. We then construct a 64×64 swapping matrix $\mathbf{\Lambda}$. The matrix is diagonal with entries of 1 where there are entries in the input state we would like to keep and entries of 0 where there are entries in the input state we would like to swap (see the Appendix). We then construct a second swapping matrix $\mathbf{I} - \mathbf{\Lambda} = \mathbf{\Gamma}$. A unitary matrix can now be constructed from the swapping matrices, $\mathbf{\Lambda}$ and $\mathbf{\Gamma}$, and $\mathbf{T}_{add}$

$$\mathbf{U} = (\mathbf{\Gamma} + \mathbf{\Lambda} \cdot \mathbf{T}_{add}) \cdot (\mathbf{\Lambda} + \mathbf{\Gamma} \cdot \mathbf{T}_{add})^{-1}. \tag{15}$$

This unitary matrix is very useful for studying the dynamics of the network and computing optimal states of the network as the reflection parameter b is varied.

One way to look at the interconnectedness of the quantum network is to study the behavior of the eigenvalues of the quantum network. In Fig. 8 we show their behavior as we increase the reflection parameter b. We find that the eigenvalues of $\mathbf{U}$ show a rapid spreading throughout the unit circle (Fig. 8). This eigenvalue spreading indicates that the directional properties of the quantum network are breaking down. The unitary matrices corresponding to adder networks with the $\sqrt{\text{NOT}}$ gate shows similar eigenvalue spreading.

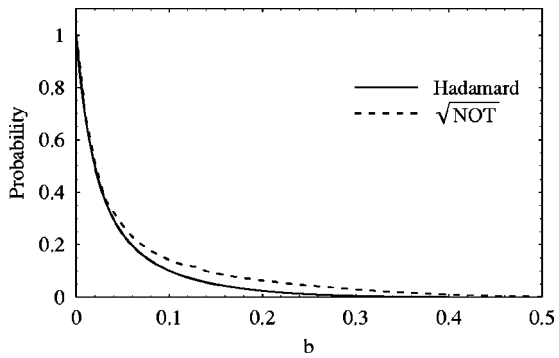

FIG. 9. A plot of the output probability of the correct answer state $|1, 0, 1\rangle$ changing with reflection parameter b. Solid lines represent the Hadamard adder and dashed lines represent the $\sqrt{\text{NOT}}$ adder.

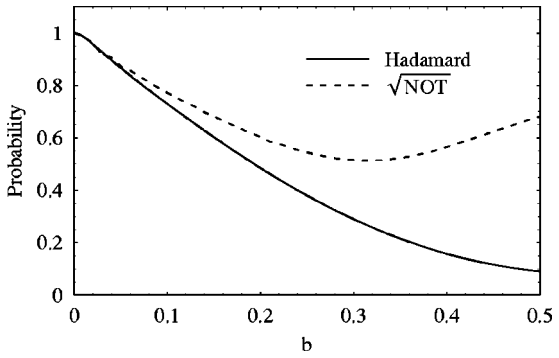

FIG. 10. A plot of the input probability of the perfect input state $|1, 1, 0\rangle$ changing with reflection parameter b. Solid lines represent the Hadamard adder and dashed lines represent the $\sqrt{\text{NOT}}$ adder.

B. Stationary states of the network

The states of the system on which **U** acts we call *primary* states. The states which result from the action of **U** on the primary states we call *resultant* states. Due to the unitarity of **U**, the primary state and the resultant state for a network, with a given reflection parameter b, will have the same norm. To find stationary state solutions of the network which allow the adder to function most efficiently, we first must find the eigenvectors of **U**. We expand a primary state in terms of the eigenvectors of **U**, $|\phi_i\rangle$, with unknown expansion coefficients α_i

$$|\Psi_{act}\rangle = \alpha_1|\phi_1\rangle + \alpha_2|\phi_2\rangle + \cdots + \alpha_{64}|\phi_{64}\rangle. \tag{16}$$

U acting upon the expanded primary state gives the resultant state written as an expansion in eigenvectors where for each eigenstate $|\phi_i\rangle$ the expansion coefficient is the expansion coefficient of the primary state multiplied by the eigenvalue ϵ_i associated with that eigenvector,

$$|\Psi_{res}\rangle = \alpha_1\epsilon_1|\phi_1\rangle + \alpha_2\epsilon_2|\phi_2\rangle + \cdots + \alpha_{64}\epsilon_{64}|\phi_{64}\rangle. \tag{17}$$

We find a set of equations for the expansion coefficients which are solved for a given set of required input and output states.

The boundary conditions that we impose on the system involve setting the incoming probability into the network. There should be no electron probability incoming from the output side of the network. The perfect input state for our network is unit current incoming in the input state $|1, 1, 0\rangle$. Once the primary and resultant states are found, we employ the swapping matrices to recover the input and output states. All calculations are performed for values of $0 \leqslant b \leqslant 0.5$. For $b > 0.5$ the calculations become unstable.

We find that when there is no reflection present both quqit adder networks give the same result as the corresponding qubit adder network. However, when reflection is present it is not possible to find simultaneously an output state with no incoming probability and an input state with incoming probability in only the $|1,1,0\rangle$ state. We choose to relax our input and output states in such a way as to find solutions which maintain the condition of no incoming probability from the output side of the network but allow a small change to the incoming probability on the input side. In Fig. 9, we show the probability of finding the correct output state as a function of b. In Fig. 10, we show the probability of having the the correct input as a function b.

The probability of finding the correct output of the quqit adder decreases rapidly with b and depends on the type of adder. For an adder constructed with Hadamard gates the probability of finding the correct output is less than $\frac{1}{2}$ when $b > 0.020$. In the case of an adder built using $\sqrt{\text{NOT}}$ gates, the probability of finding the correct output is less than $\frac{1}{2}$ when $b > 0.023$.

The ratio of outgoing electron probability in two states of a single quqit is found by

$$\frac{|e_0|^2}{|e_1|^2} = \frac{\langle\Psi_{out}|(|0\rangle\langle 0|)|\Psi_{out}\rangle}{\langle\Psi_{out}|(|1\rangle\langle 1|)|\Psi_{out}\rangle}. \tag{18}$$

Once all of the ratios of the probabilities outgoing in states of a single a quqit are known the total outgoing probability is normalized to unity and the individual probabilities are found. The same procedure is performed for the incoming probabilities of single quqits. There are no rotation gates on quqit A in either adder network, and as a result there is no reflection in quqit A. We discuss only the results for quqit B and quqit C as quqit A maintains perfect input and output. We find a rapid decrease in the amount of probability leaving

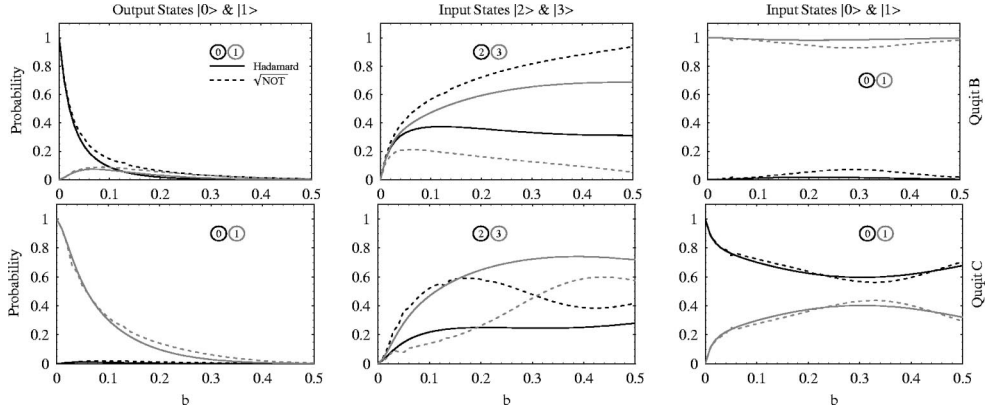

FIG. 11. A plot of the probability entering and leaving the individual quqits B and C. Solid lines represent the Hadamard adder and dashed lines represent the $\sqrt{\text{NOT}}$ adder.

the system in the correct states as the reflection parameter b is increased (Fig. 11). The change in incoming probabilities is somewhat slower and less defined. The input boundary conditions on quqit C are relaxed most as quqit C is the carry quqit and often under the most algorithmic control.

V. CONCLUSIONS

It is possible to implement a simple adder network with electron waveguides. The fidelity of the calculation decreases rapidly as the reflection is increased. Within the limits of the calculation an adder network constructed with Hadamard gates allows a probability greater than $\frac{1}{2}$ of finding the correct answer when the a reflection parameter $b \leqslant 0.020$. This corresponds to finding a single Hadamard gate of fidelity $F \geqslant 0.960$. An adder network constructed with $\sqrt{\text{NOT}}$ gates allows a probability greater than $\frac{1}{2}$ of finding the correct answer when the reflection parameter $b \leqslant 0.023$ corresponding to a single gate of fidelity $F \geqslant 0.954$.

ACKNOWLEDGMENTS

The authors thank the Robert A. Welch Foundation (Grant No. F-1051) and the Engineering Research Program of the Office of Basic Energy Sciences at the U.S. Department of Energy (Grant No. DE-FG03-94ER14465) for support of this work. L.E.R. thanks the U.S. Office of Naval Research (Grant No. N00014-03-1-0639) for partial support of this work.

APPENDIX

Equations (1)–(3) are multiplied together and rearranged to find a total probability conservation equation:

$$
\begin{aligned}
&|a_1b_1c_1|^2 + |a_1b_1c_0|^2 + |e_1f_1g_u|^2 + |e_1f_1g_d|^2 + |a_1b_0c_1|^2 + |a_1b_0c_0|^2 + |e_1f_0g_u|^2 + |e_1f_0g_d|^2 + |e_1f_ug_1|^2 + |e_1f_ug_0|^2 + |a_1b_uc_u|^2 \\
&\quad + |a_1b_uc_d|^2 + |e_1f_dg_1|^2 + |e_1f_dg_0|^2 + |a_1b_dc_u|^2 + |a_1b_dc_d|^2 + |a_0b_1c_1|^2 + |a_0b_1c_0|^2 + |e_0f_1g_u|^2 + |e_0f_1g_d|^2 + |a_0b_0c_1|^2 \\
&\quad + |a_0b_0c_0|^2 + |e_0f_0g_u|^2 + |e_0f_0g_d|^2 + |e_0f_ug_1|^2 + |e_0f_ug_0|^2 + |a_0b_uc_u|^2 + |a_0b_uc_d|^2 + |e_0f_dg_1|^2 + |e_0f_dg_0|^2 + |a_0b_dc_u|^2 \\
&\quad + |a_0b_dc_d|^2 + |e_uf_1g_1|^2 + |e_uf_1g_0|^2 + |a_ub_1c_u|^2 + |a_ub_1c_d|^2 + |e_uf_0g_1|^2 + |e_uf_0g_0|^2 + |a_ub_0c_u|^2 + |a_ub_0c_d|^2 + |a_ub_uc_1|^2 \\
&\quad + |a_ub_uc_0|^2 + |e_uf_ug_u|^2 + |e_uf_ug_d|^2 + |a_ub_dc_1|^2 + |a_ub_dc_0|^2 + |e_uf_dg_u|^2 + |e_uf_dg_d|^2 + |e_df_1g_1|^2 + |e_df_1g_0|^2 + |a_db_1c_u|^2 \\
&\quad + |a_db_1c_d|^2 + |e_df_0g_1|^2 + |e_df_0g_0|^2 + |a_db_0c_u|^2 + |a_db_0c_d|^2 + |a_db_uc_1|^2 + |a_db_uc_0|^2 + |e_df_ug_u|^2 + |e_df_ug_d|^2 + |a_db_dc_1|^2 \\
&\quad + |a_db_dc_0|^2 + |e_df_dg_u|^2 + |e_df_dg_d|^2 \\
&= |e_1f_1g_1|^2 + |e_1f_1g_0|^2 + |a_1b_1c_u|^2 + |a_1b_1c_d|^2 + |e_1f_0g_1|^2 + |e_1f_0g_0|^2 + |a_1b_0c_u|^2 + |a_1b_0c_d|^2 + |a_1b_uc_1|^2 + |a_1b_uc_0|^2 \\
&\quad + |e_1f_ug_u|^2 + |e_1f_ug_d|^2 + |a_1b_dc_1|^2 + |a_1b_dc_0|^2 + |e_1f_dg_u|^2 + |e_1f_dg_d|^2 + |e_0f_1g_1|^2 + |e_0f_1g_0|^2 + |a_0b_1c_u|^2 + |a_0b_1c_d|^2 \\
&\quad + |e_0f_0g_1|^2 + |e_0f_0g_0|^2 + |a_0b_0c_u|^2 + |a_0b_0c_d|^2 + |a_0b_uc_1|^2 + |a_0b_uc_0|^2 + |e_0f_ug_u|^2 + |e_0f_ug_d|^2 + |a_0b_dc_1|^2 + |a_0b_dc_0|^2 \\
&\quad + |e_0f_dg_u|^2 + |e_0f_dg_d|^2 + |a_ub_1c_1|^2 + |a_ub_1c_0|^2 + |e_uf_1g_u|^2 + |e_uf_1g_d|^2 + |a_ub_0c_1|^2 + |a_ub_0c_0|^2 + |e_uf_0g_u|^2 + |e_uf_0g_d|^2 \\
&\quad + |e_uf_ug_1|^2 + |e_uf_ug_0|^2 + |a_ub_uc_u|^2 + |a_ub_uc_d|^2 + |e_uf_dg_1|^2 + |e_uf_dg_0|^2 + |a_ub_dc_u|^2 + |a_ub_dc_d|^2 + |a_db_1c_1|^2 + |a_db_1c_0|^2 \\
&\quad + |e_df_1g_u|^2 + |e_df_1g_d|^2 + |a_db_0c_1|^2 + |a_db_0c_0|^2 + |e_df_0g_u|^2 + |e_df_0g_d|^2 + |e_df_ug_1|^2 + |e_df_ug_0|^2 + |a_db_uc_u|^2 + |a_db_uc_d|^2 \\
&\quad + |e_df_dg_1|^2 + |e_df_dg_0|^2 + |a_db_dc_u|^2 + |a_db_dc_d|^2. \qquad \text{(A1)}
\end{aligned}
$$

We identify those amplitudes in each state that must be swapped and construct two swapping matrices $\mathbf{\Lambda}$ and $\mathbf{\Gamma}$. Λ is a diagonal matrix with entries

$$
\begin{aligned}
&\text{diag}(\mathbf{\Lambda}) \\
&\quad = (1,1,0,0,1,1,0,0,0,0,1,1,0,0,1,1,1,1,0,0,1,1,0,0,0,1,1,0,0,1,1,0,0,1,1,0,0,1,1,1,1,0,0,1,1,0,0,0,0, \\
&\qquad 1,1,0,0,1,1,1,1,0,0,1,1,0,0). \qquad \text{(A2)}
\end{aligned}
$$

[1] Radu Ionicioiuu, Gehan Amaratunga, and Florin Udrea, Int. J. Mod. Phys. B **15**, 125 (2001).

[2] Gursoy B. Akguc, Linda E. Reichl, Anil Shaji, and Michael G. Snyder, Phys. Rev. A **69**, 042303 (2004).

[3] M. A. Nielsen and I. L. Chuang, *Quantum Computation and Quantum Information* (Cambridge University Press, Cambridge, U.K., 2000).

[4] A. Ekert, P. Hayden, and H. Inamori, e-print quant-ph/0011013.

[5] P. W. Shor, in *Proceedings of the 35th Annual Symposium on*

the Foundations of Computer Science (IEEE Computer Society Press, Los Alamitos, CA, 1994), p. 124.
[6] V. Vedral, A. Barenco, and A. Ekert, Phys. Rev. A **54**, 147 (1996).
[7] S. Datta, *Electronic Transport in Mesoscopic Systems* (Cambridge University Press, Cambridge, U.K., 1995).
[8] J. Harris, R. Akis, and D. K. Ferry, Appl. Phys. Lett. **79**, 2214 (2001).
[9] J. P. Bird, R. Akis, D. K. Ferry, A. P. S. de Moura, Y.-C. Lai, and K. M. Indlekofer, Rep. Prog. Phys. **66**, 583 (2001).